

Electronic Supplementary Information (ESI)

Halide-mediated Ag-Zn batteries in alkaline electrolytes

Jiajie Shen,[#] Wenjiao Ma,[#] Jianhui Jin, Huijian Wang, Xiao Liang*

State Key Laboratory of Chemo and Biosensing, Joint International
Research Laboratory of Energy Electrochemistry, College of Chemistry
and Chemical Engineering, Hunan University, Changsha 410082, China.

E-mail: xliang@hnu.edu.cn

[#] These authors contributed equally.

Experimental section

All reagents and starting materials were used as received without any further purification. Potassium hydroxide (KOH), nano zinc oxide (ZnO), potassium chloride (KCl), potassium bromide (KBr), and potassium iodide (KI) were purchased from Aladdin. PEO and PVDF were purchased from Sigma-Aldrich. Silver powder was analytical-grade micron-sized silver powder.

Preparation of self-standing electrode

PVDF and PEO were dissolved in NMP, and the resulting polymer solution was mixed with short carbon fibers, Super P, and silver powder. After thorough mixing, the mixture was poured into a polytetrafluoroethylene mold and dried overnight in an oven at 80 °C to obtain a self-supporting silver electrode. The weight ratio of PVDF, PEO, carbon, and silver powder was 1.5:1.5:2:5.

Characterization of Physicochemical Properties

Powder X-ray diffraction (XRD) was performed on D8 ADVANCE with Cu K α radiation and a scan rate of 10 °C min⁻¹ at 40 KV, 30 mA. Scanning electron microscope (SEM) was carried out on MIRA4 LMH. ICP-MS analysis was performed on an Agilent 7700.

Electrochemical measurements

Swagelok type was assembled with zinc foil anode (0.1 mm thickness, 12 mm in diameter), glass fiber separator (Whatman GF/A, 12 mm in diameter) and self-standing silver cathode (12 mm in diameter) with 100 μ L electrolyte. Impedance measurements of the cathode were conducted using a three-electrode system on a VMP-3 workstation (Bio-Logic). The cathode consisted of a self-supported silver electrode, the anode was a platinum mesh, and a silver/silver chloride electrode (with a reference potential of +0.199 V vs. standard hydrogen electrode, SHE) was used as the reference electrode. A perturbation of 100 μ A was applied over a frequency range from 10 mHz to 0.1 MHz. Cyclic voltammetry measurements were performed on an electrochemical workstation (Gamry, USA). The GITT test was conducted within the voltage range of 1.2 to 1.6 V, consisting of a series of current pulses (1.5 mA cm²) applied for 5 minutes, followed by a 30 minutes relaxation period.

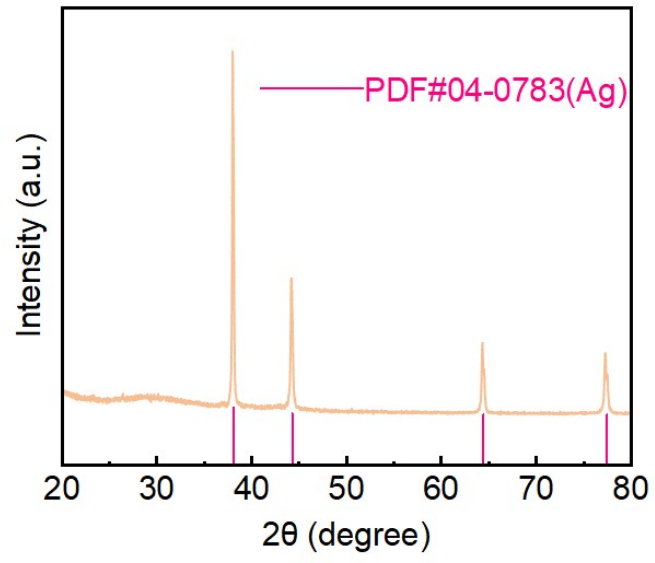


Fig. S1 XRD pattern of the initial state electrode.

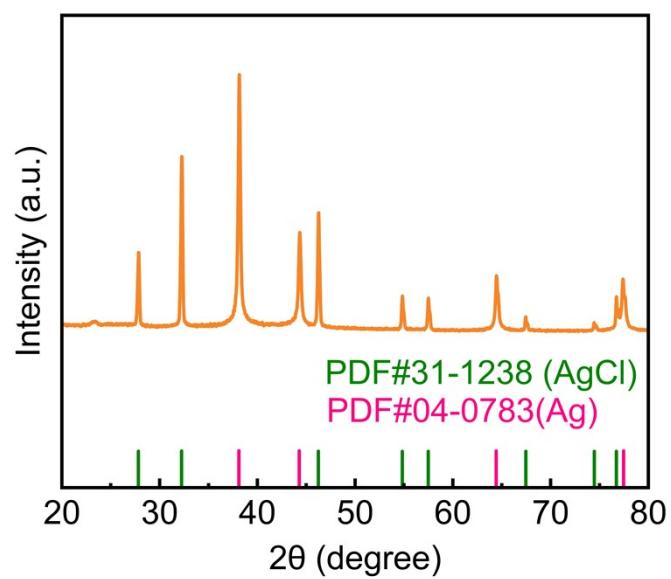


Fig. S2 XRD pattern of charged state electrode in KOCl.

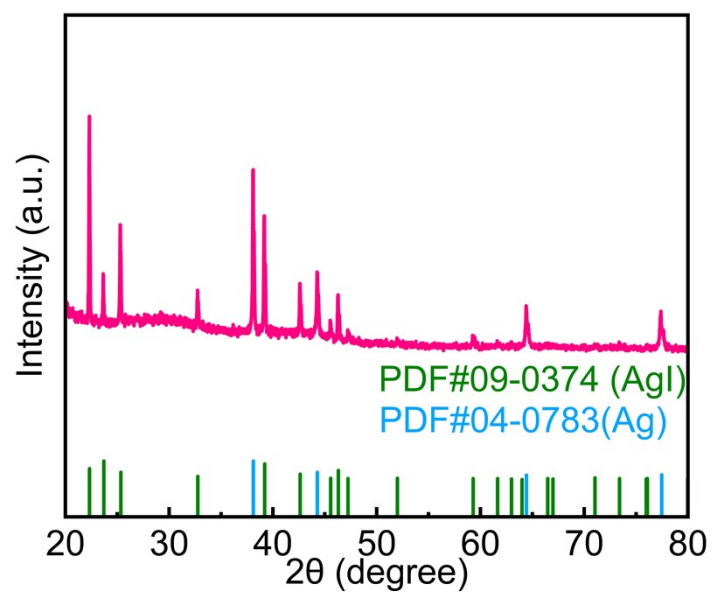


Fig. S3 XRD pattern of charged state electrode in KOI.

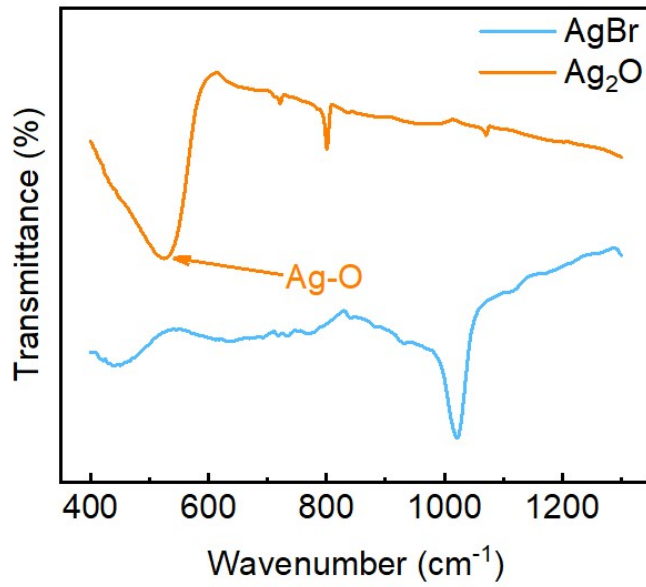


Fig. S4 FTIR spectra of Ag₂O powder and the charged silver electrode using KOB_r electrolyte.

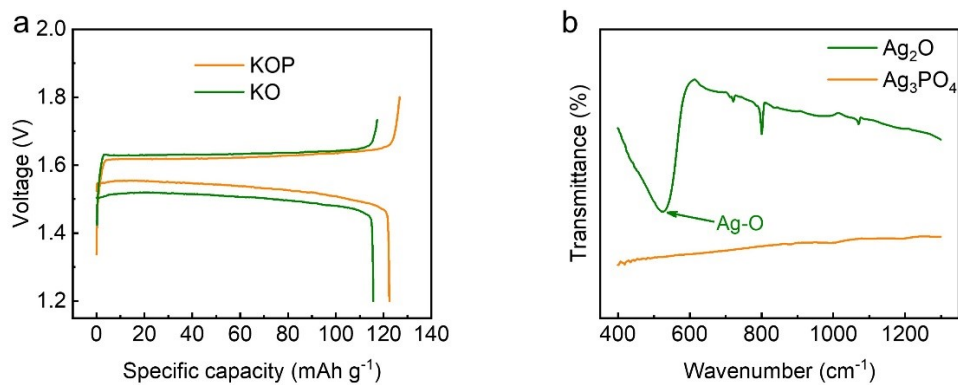


Fig. S5 (a) Charge–discharge profiles of batteries using KO electrolyte and KOP electrolyte (KO with 0.2 M K₃PO₄); (b) FTIR spectra of Ag₂O powder and the charged silver electrode using KOP electrolyte.

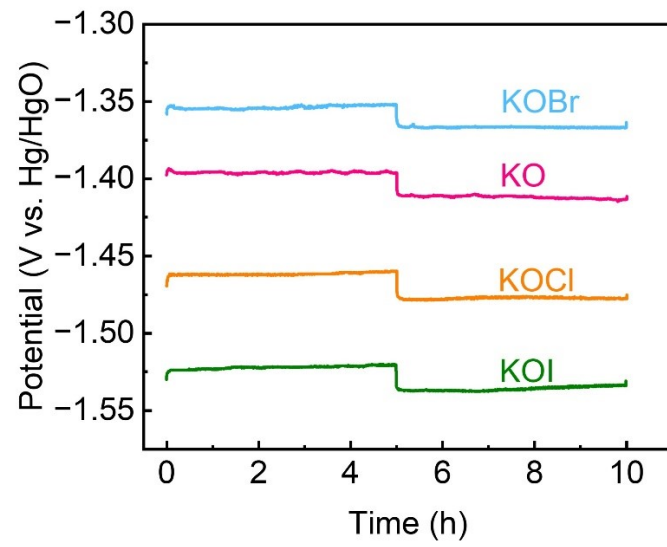


Fig. S6 Time-voltage curve of Zn anode using different electrolytes.

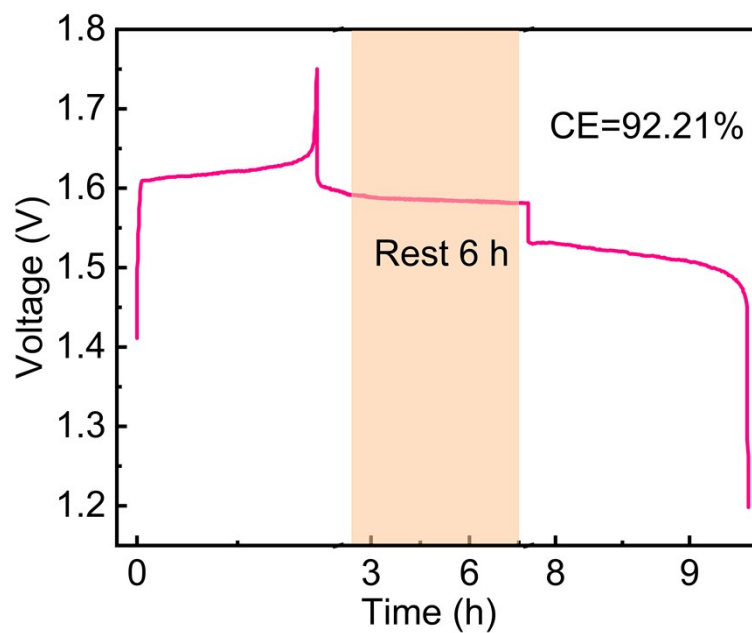


Fig. S7 Self-discharge test of the battery using KO electrolyte after 6 hours of rest.

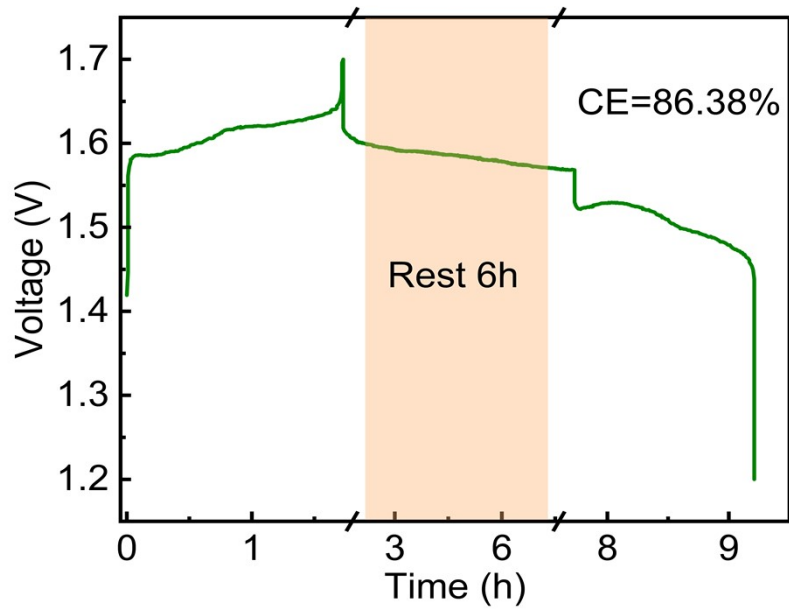


Fig. S8 Self-discharge test of the battery using KOCl electrolyte after 6 hours of rest.

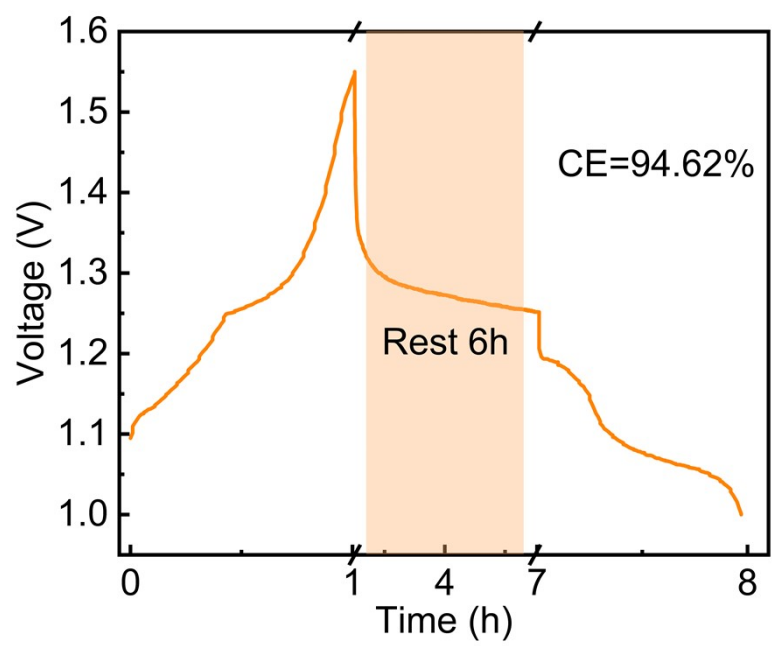


Fig. S9 Self-discharge test of the battery using KOI electrolyte after 6 hours of rest.

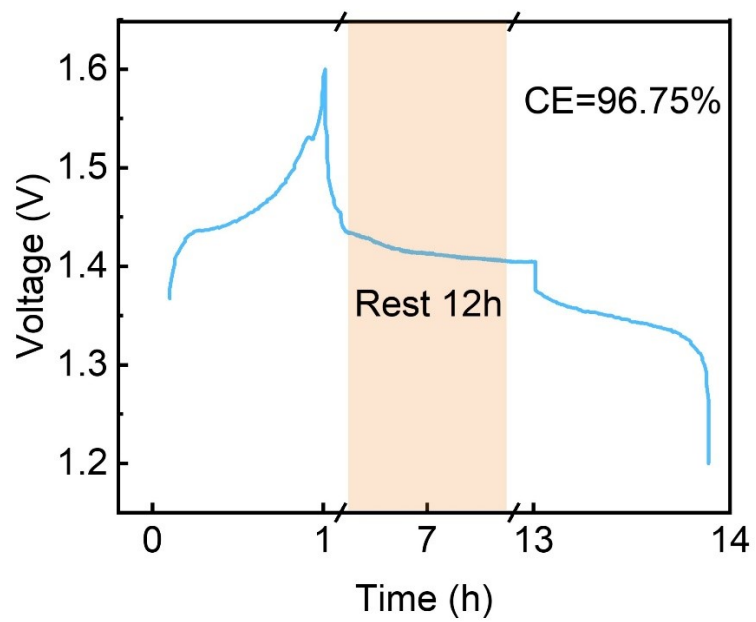


Fig. S10 Self-discharge test of the battery using KOBr electrolyte after 12 hours of rest.

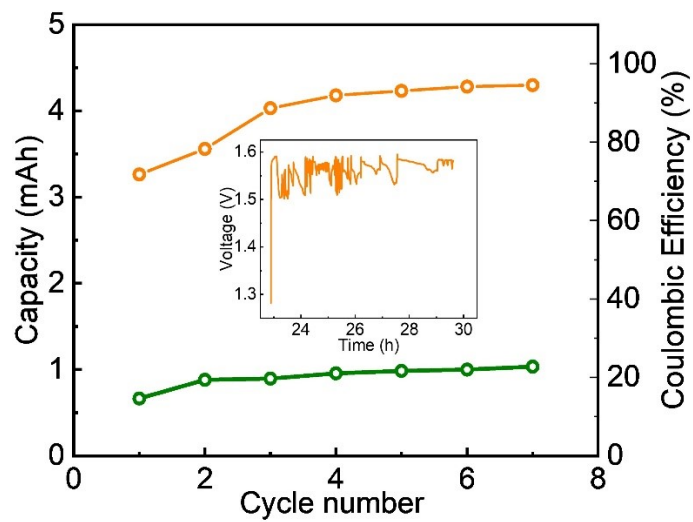


Fig. S11 Cycling performance and voltage fluctuations at battery failure using KOCl electrolyte.

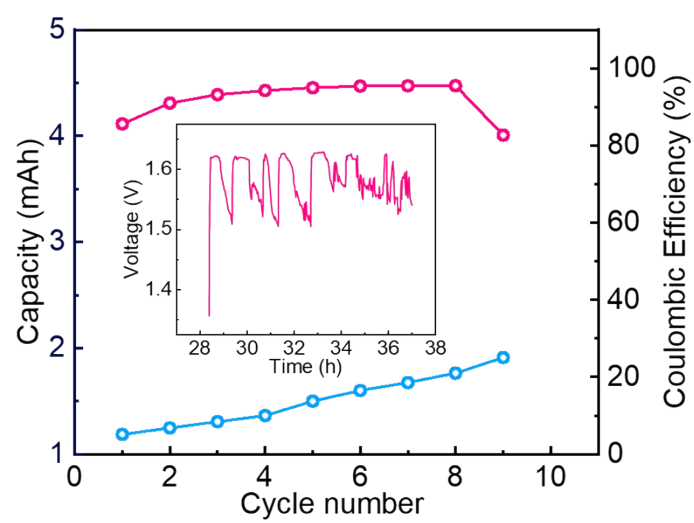


Fig. S12 Cycling performance and voltage fluctuations at battery failure using KO electrolyte.

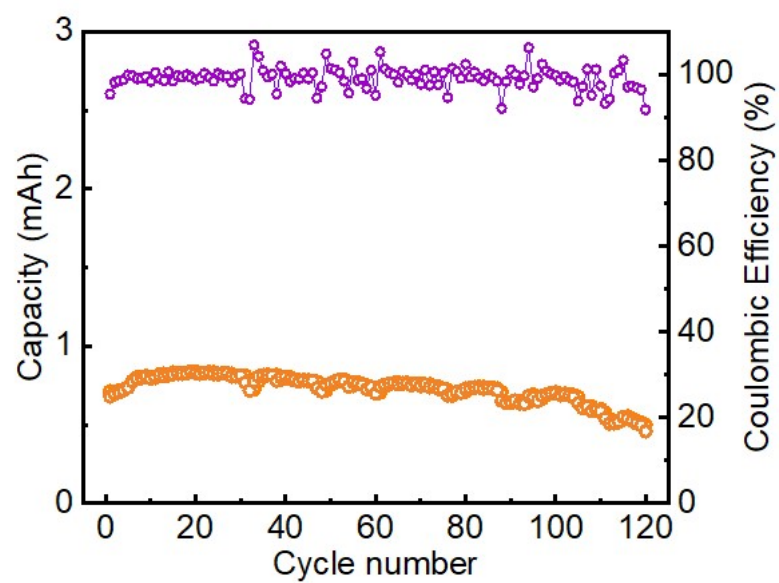


Fig. S13 Cycling performance of the battery using KOI electrolyte.

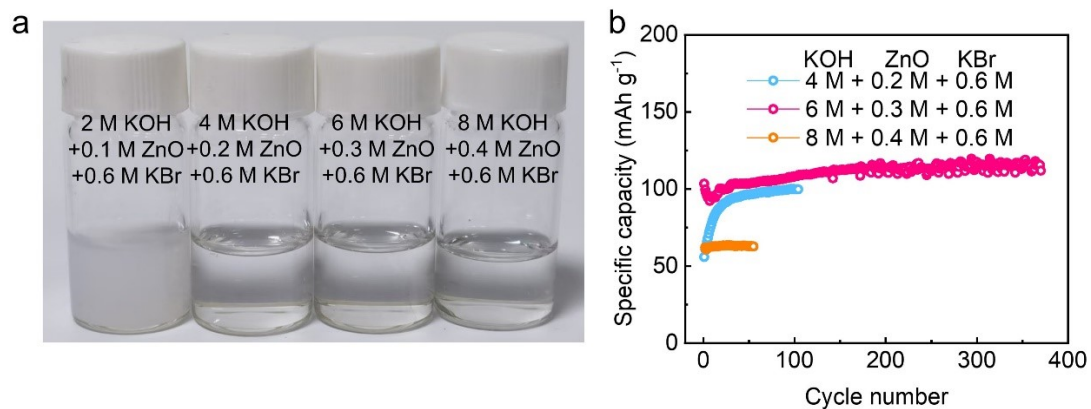


Fig. S14 (a) Images of KOBr solutions with different KOH concentrations; (b) Cycling performance of halide-mediated batteries using electrolytes with varying KOH concentrations.

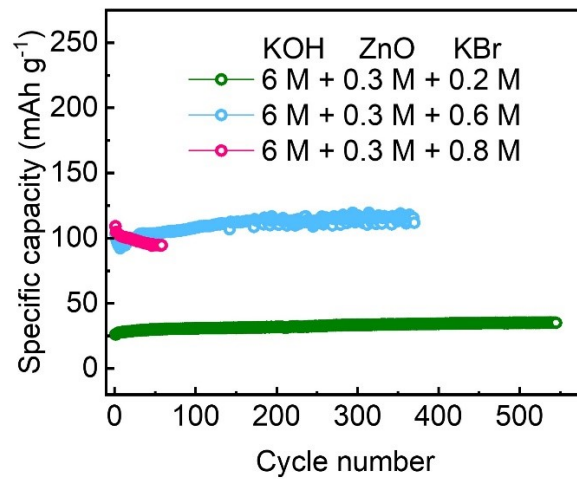


Fig. S15 The cycle performance of batteries using electrolytes with different Br⁻ concentrations.

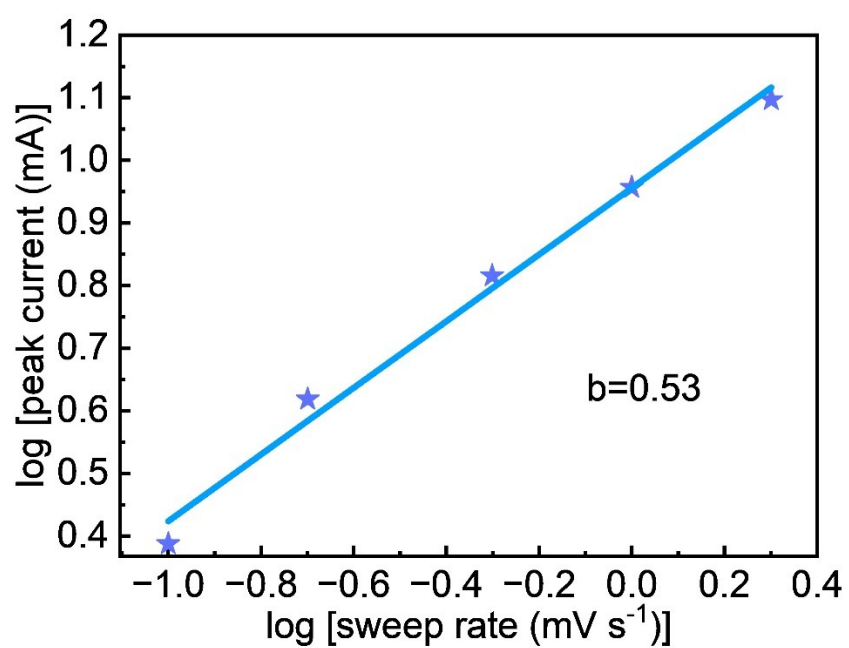


Fig. S16 The b value of the CV at different scan rates in the KOB₃ electrolyte.

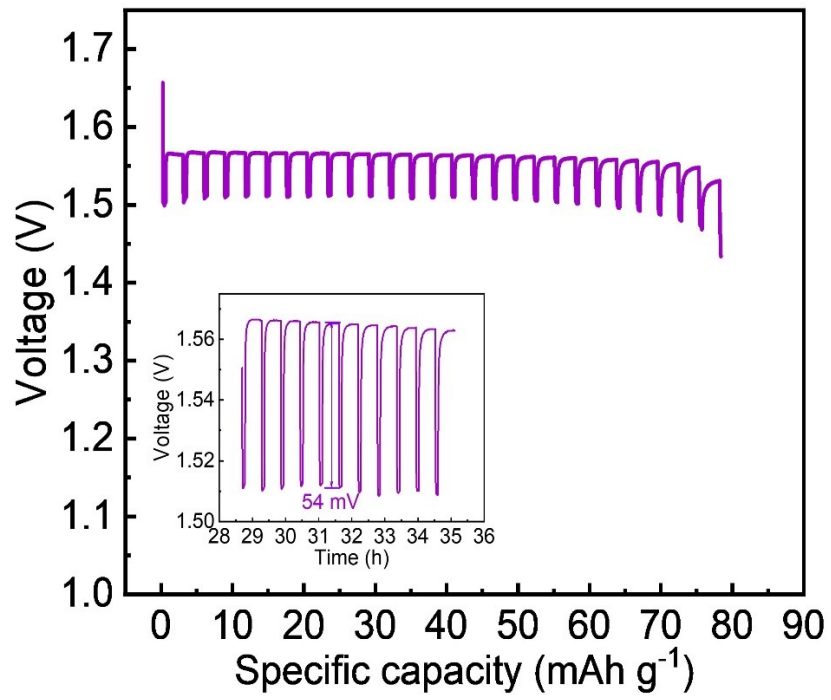


Fig. S17 GITT analysis of the battery using KO electrolyte and the corresponding magnified view.

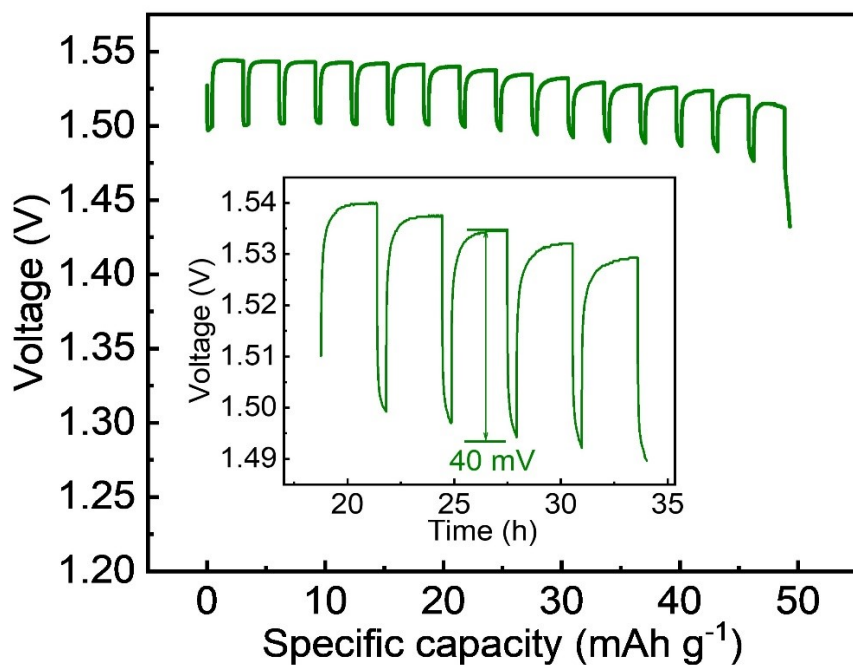


Fig. S18 GITT analysis of the battery using KOCl electrolyte and the corresponding magnified view.

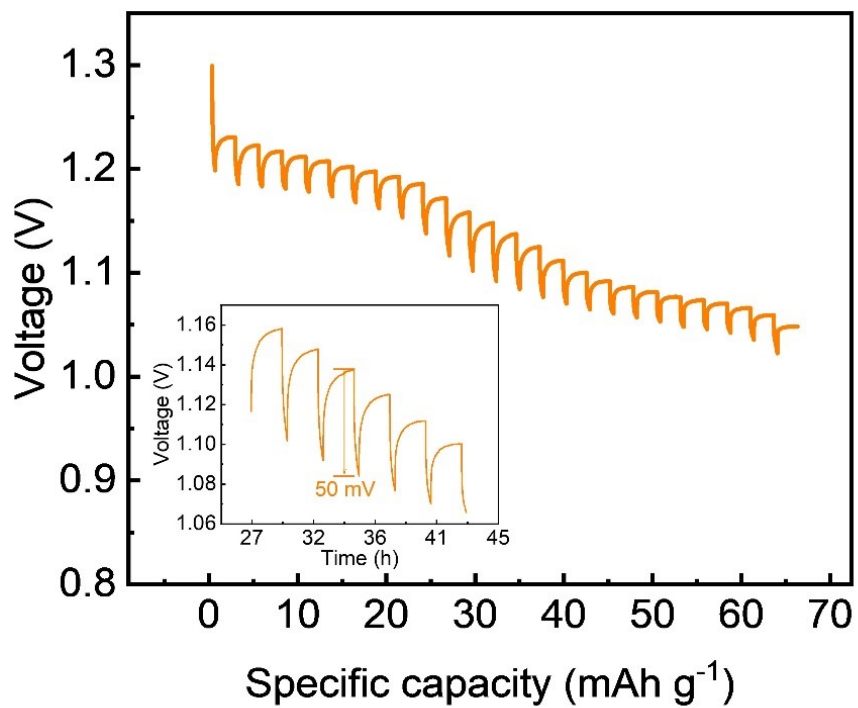


Fig. S19 GITT analysis of the battery using KOI electrolyte and the corresponding magnified view.

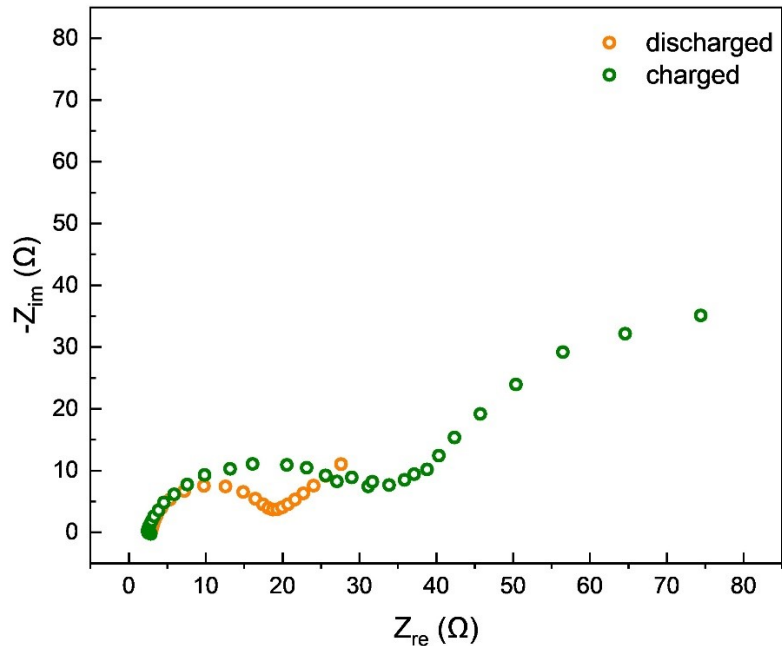


Fig. S20 EIS test of the silver electrode using KO electrolyte in the charged and discharged states.

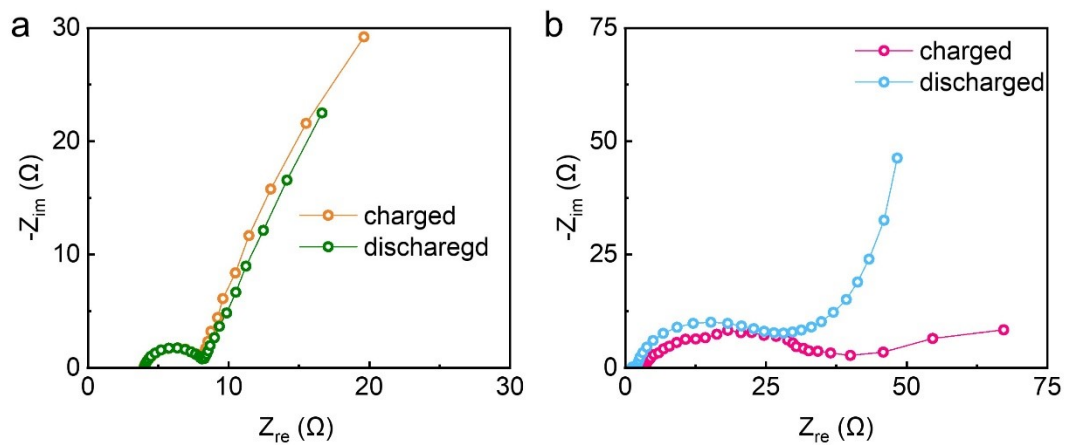


Fig. S21 EIS tests of the silver electrode using (a) KOCl and (b) KOI electrolytes in the charged and discharged states.

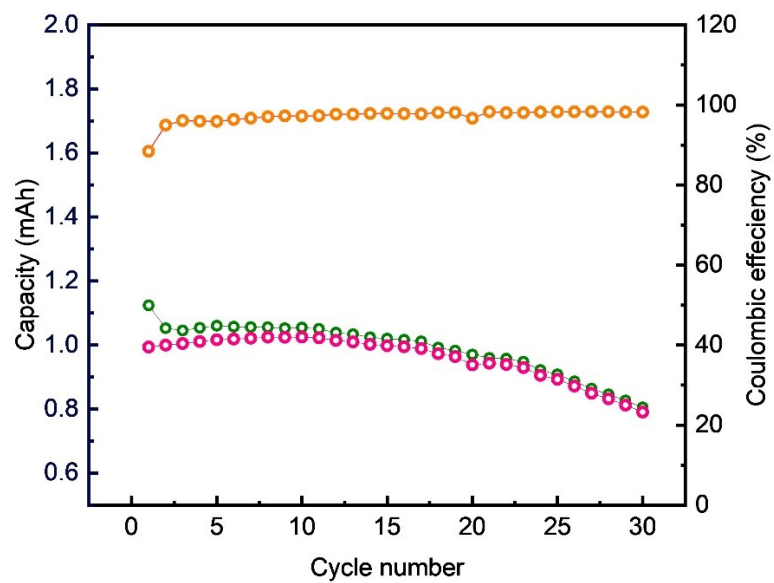


Fig. S22 The capacity fading of battery using conventional Ag electrode.

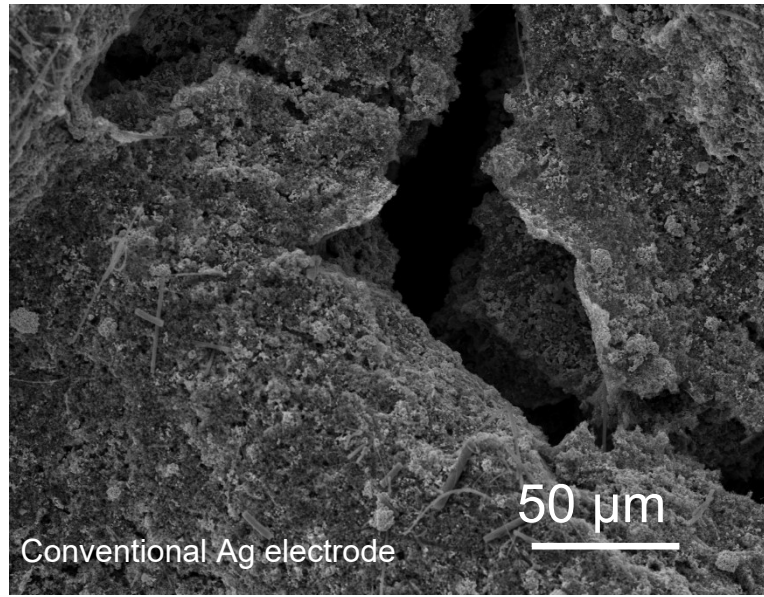


Fig. S23 SEM image of conventional Ag electrode after cycling.

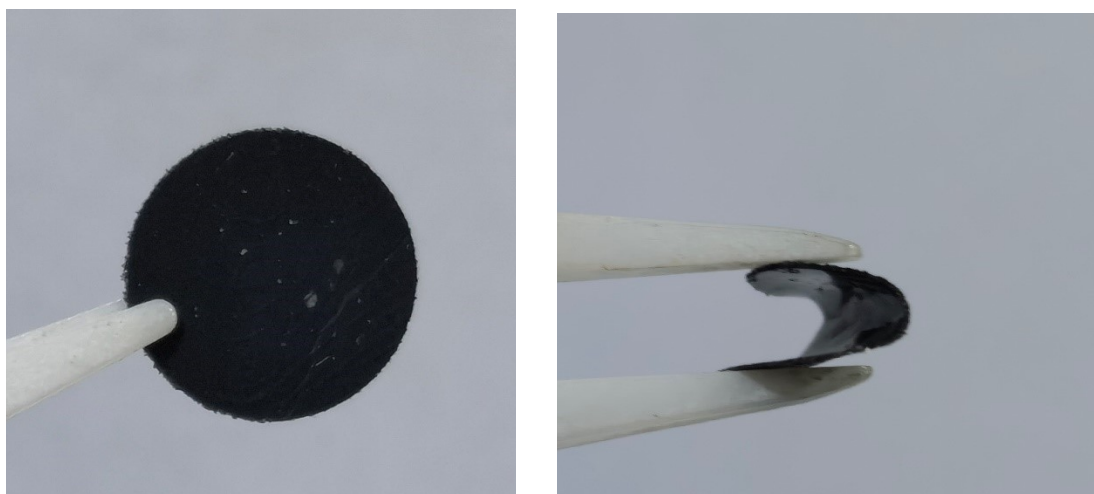


Fig. S24 Optical photograph of the self-supporting electrode.

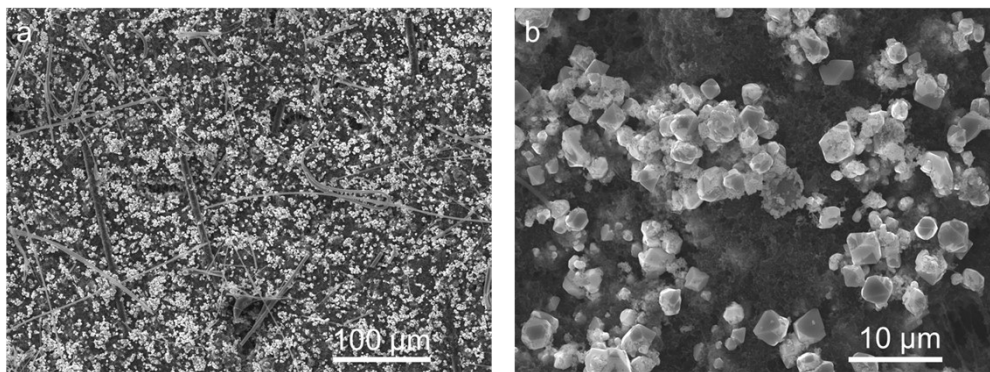


Fig. S25 Surface SEM image of self-standing electrode.

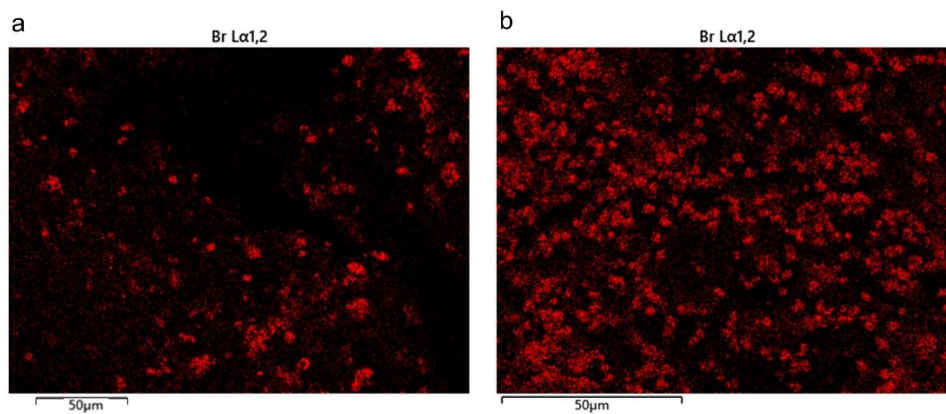


Fig. S26 EDS mapping of (a) conventional Ag electrode and (b) self-standing electrode in the charged state.

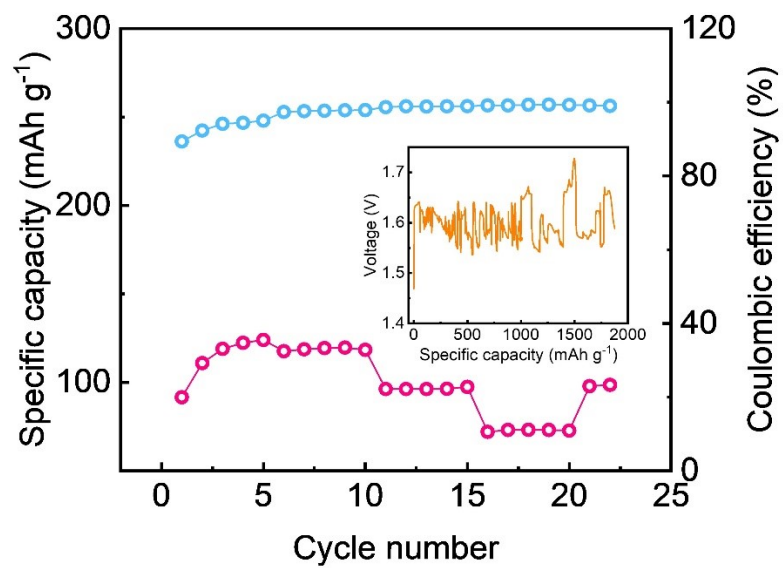


Fig. S27 Rate performance of battery in KO electrolyte.

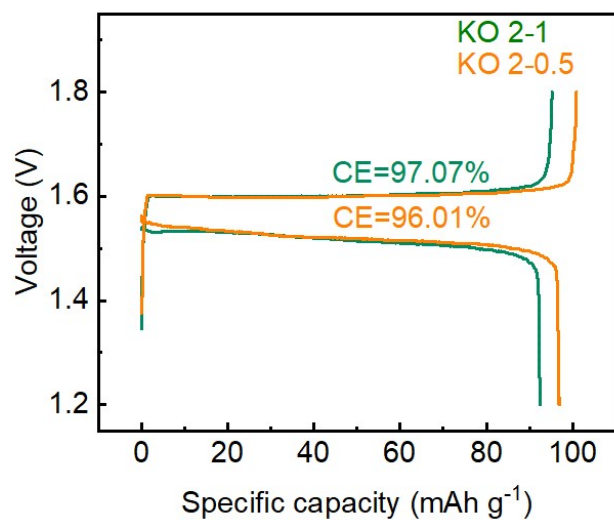


Fig. S28 The fast charge-slow discharge performance of batteries using KO electrolyte.

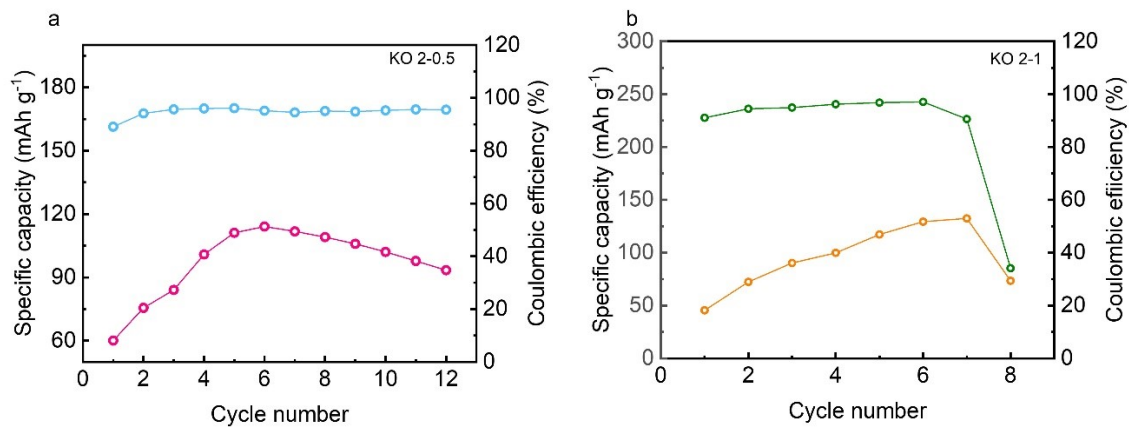


Fig. S29 The cycling performance of batteries using KO electrolyte.

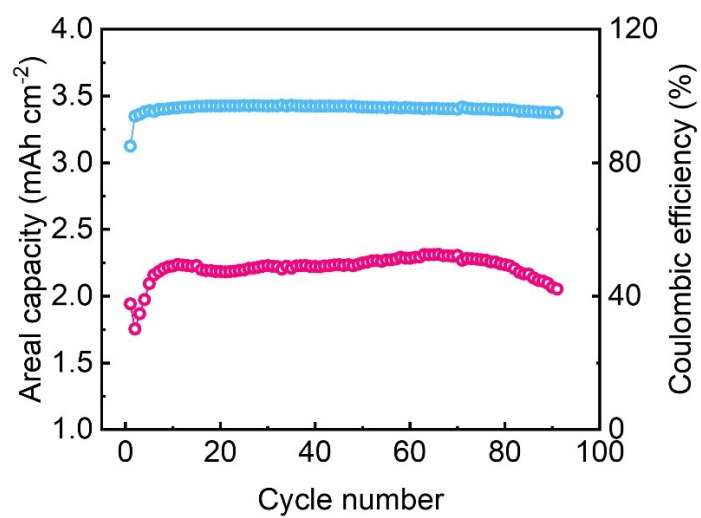


Fig. S30 Cycling performance of halide-mediated Ag-Zn battery with high areal capacity.